Geophysical Research Letters

Supporting Information for

Effect of a thin weak layer at around the 660-km discontinuity on subducting slab morphology in the mantle transition zone

Zhong-Hai Li [1], Ling Chen [2,3]

[1] Key Laboratory of Computational Geodynamics, College of Earth and Planetary Sciences, University of Chinese Academy of Sciences, Beijing, China.

[2] State Key Laboratory of Lithospheric Evolution, Institute of Geology and Geophysics, Chinese Academy of Sciences, Beijing, China

[3] CAS Center for Excellence in Tibetan Plateau Earth Sciences, Beijing, China

Contents of this file

Introduction

This supporting Information includes:

Text S1 summarizes the numerical methods.

Figure S1 shows the previous inferences of depth-dependent effective mantle viscosity.

Table S1 shows the viscous flow laws used in the numerical experiments.

Table S2 shows the material properties used in the numerical experiments.

Text S1.

1. Governing equations

The numerical models are conducted with the code I2VIS, which combines the finite difference and marker-in-cell methods (*Gerya, 2010*). Three sets of conservation equations (mass, momentum and energy) with the constitutive relationships are solved in the two-dimensional regime.

(1) Stokes equation:

$$\frac{\partial \sigma'_{ij}}{\partial x_j} = \frac{\partial P}{\partial x_i} - g_i \rho(C, M, P, T) \quad (i, j = 1, 2)$$

Where σ' is the deviatoric stress tensor; x is the spatial coordinate; g is the gravitational acceleration; the density ρ depends on composition (C), melt fraction (M), dynamic pressure (P) and temperature (T). For a specific rock type:

$$\rho = \rho_{\text{solid}} - M(\rho_{\text{solid}} - \rho_{\text{molten}})$$
$$\rho_{\text{solid|molten}} = \rho_0 \left[1 - \alpha(T - T_0)\right]\left[1 + \beta(P - P_0)\right]$$

Where ρ_0 is the density under the reference condition with P_0 = 0.1 MPa and T_0 = 298 K. α and β are the thermal expansion coefficient and the compressibility coefficient, respectively. Rock density is further corrected for phase transitions.

The constitutive relationship is shown below:

$$\sigma'_{ij} = 2\eta_{\text{eff}} \dot{\varepsilon}_{ij}$$
$$\dot{\varepsilon}_{ij} = \frac{1}{2}\left(\frac{\partial v_i}{\partial x_j} + \frac{\partial v_j}{\partial x_i}\right)$$

Where $\dot{\varepsilon}$ and v are the deviatoric strain rate tensor and velocity vector, respectively. η_{eff} is the effective viscosity.

(2) Incompressible continuity equation:

$$\frac{\partial v_i}{\partial x_i} = 0$$

(3) Energy equation:

$$\rho C_p \left(\frac{DT}{Dt}\right) = -\frac{\partial q_i}{\partial x_i} + H$$
$$q_i = -k(C, P, T)\frac{\partial T}{\partial x_i}$$

Where DT/Dt is the substantive time derivative of temperature; C_p is the effective isobaric heat capacity; q is the thermal heat flux; H represents the heat generations, including radioactive

heat production (H_r), adiabatic heating (H_a) and shear heating (H_s). k is the thermal conductivity, dependent on composition (C), pressure (P) and temperature (T).

2. Visco-Plastic-Peierls rheology

(1) Viscous flow law of crustal rocks:

The viscosities of both the continental and oceanic crustal rocks are calculated according to the flow laws of *Ranalli* (1995):

$$\eta_{\text{ductile}} = \frac{1}{2}(A_R)^{-\frac{1}{n}}(\dot{\varepsilon}_{II})^{\frac{1-n}{n}}\exp(\frac{E+PV}{nRT})$$

Where A_R (pre-exponential factor), n (creep exponent), E (activation energy) and V (activation volume) are experimentally determined flow law parameters (A* and B* in Table S1); $\dot{\varepsilon}_{II} = (0.5\dot{\varepsilon}_{ij}\dot{\varepsilon}_{ij})^{1/2}$ is the second invariant of strain rate tensor; R is the gas constant.

(2) Viscous flow law of mantle rocks:

The rheology of mantle rocks is defined according to *Karato and Wu* (*1993*), integrating both diffusion and dislocation creep:

$$\eta_{\text{diffusion | dislocation}} = \frac{1}{2}(A_K)^{-\frac{1}{n}}u\left(\frac{d}{b}\right)^{\frac{m}{n}}(\dot{\varepsilon}_{II})^{\frac{1-n}{n}}\exp(\frac{E+PV}{nRT})$$

$$\frac{1}{\eta_{\text{ductile}}} = \frac{1}{\eta_{\text{diffusion}}} + \frac{1}{\eta_{\text{dislocation}}}$$

Where u is the shear modulus (u = 80GPa); b is the length of Burgers vector (b = 0.5nm); d is grain size (d = 1mm); m is the grain size exponent. Similarly, A_K (pre-exponential factor), n (creep exponent), E (activation energy) and V (activation volume) are flow law parameters determined from the laboratory experiments (C*, D*, E* and F* in Table S1).

(3) Plastic deformation:

The extended Drucker-Prager yield criterion is applied:

$$\eta_{\text{plastic}} = \frac{\sigma_{\text{yield}}}{2\dot{\varepsilon}_{II}}$$

$$\sigma_{\text{yield}} = C_0 + P\sin(\varphi_{\text{eff}})$$

Where σ_{yield} is the yield stress; C_0 is the residual rock strength at P=0; P is the dynamic pressure; φ_{eff} is the effective internal frictional angle, which includes the possible pore fluid/melt effects that control the brittle strength of fluid/melt containing porous or fractured media (*Li et al., 2016*).

(4) Peierls deformation:

The Peierls mechanism is also included for the deformation by low-temperature and high-stress plasticity (e.g., *Kameyama et al., 1999; Karato et al., 2001*).

$$\eta_{\text{peierls}} = \frac{1}{2A_{\text{peierls}}\sigma_{\text{II}}} \exp\left(\frac{E+PV}{RT}\left(1-\left(\frac{\sigma_{\text{II}}}{\sigma_{\text{peierls}}}\right)^{p}\right)^{q}\right)$$

Where A_{peierls}, p, and q are experimentally derived material constants. σ_{II} is the second invariant of stress tensor; σ_{peierls} is a stress value that limits the strength of the material.

(5) Integrated rheology:

The effective viscosity is defined as the minimum value among the ductile viscosity (η_{ductile}), the plastic equivalent (η_{plastic}), and the Peierls viscosity (η_{peierls}) (*Ranalli, 1995*), i.e. $\eta_{\text{eff}} = \min(\eta_{\text{ductile}}, \eta_{\text{plastic}}, \eta_{\text{peierls}})$. The final viscosity is further controlled by the prescribed cut-off values of [10^{18}, 10^{25}] Pa·s.

3. Dehydration and water migration

The numerical model includes both the connate water and mineral water. The connate water, present in sediment and oceanic upper crustal basalt, makes up to 1.0wt% at the surface and decreases to zero at 25 km:

$$X_{\text{H}_2\text{O(wt.\%)}} = (1-\frac{\Delta z}{25}) X_{\text{H}_2\text{O}(p_0)}$$

Where Δz is the depth below the surface (0-25 km); $X_{\text{H}_2\text{O}(p_0)}$ is the connate water content at the surface (1.0wt%). For the oceanic lower crust, continental crust and mantle, the connate water content is assumed to be negligible.

The mineral-bound water capacity is computed with Perple_X (*Connolly, 2005*) as a function of pressure and temperature for four typical rock types in the subduction models, i.e. sediment, basalt (oceanic upper crust), gabbro (oceanic lower crust) and hydrated mantle (*Li et al., 2019*). The representative model rock compositions, mineral phases and thermodynamic data sources are shown in *Li et al.* (2019).

The propagation of water is modeled in the form of markers: dehydration reactions lead to a release of water, which is stored in a newly generated water marker. The water markers move through the rocks with the following velocity:

$$v_{i(\text{water})} = v_i - A\left(\frac{\partial P}{\partial x_i} - g_i \rho_{\text{fluid}}\right)$$

$$A = \frac{v_{\text{percolation}}}{g_2(\rho_{\text{mantle}} - \rho_{\text{fluid}})}$$

Where $v_{i(\text{water})}$ is the fluid velocity; v_i is the local velocity of solid rock; A is a water percolation constant with a presumed standard value of $v_{\text{percolation}}$ = 10 cm/yr (e.g., *Gorczyk et al., 2007*); g_2 = 9.81 m/s^2 is the vertical gravitational acceleration component; ρ_{mantle} and ρ_{fluid} are the rock and fluid densities, respectively. When a moving water marker meets a lithology capable of absorbing water by hydration or partial melting reactions at given P–T conditions and rock composition, the water will be consumed.

4. Partial melting

Partial melting of both the crustal and mantle rocks is implemented. For the mantle rocks, the water-content-dependent parameterization of *Katz et al.* (2003) is applied, which is however limited to the depths of <300 km, because this model is inaccurate when extending to larger pressure. On the other hand, for a given crustal rock type, the volumetric degree of melting is assumed to be a linear function of temperature:

$$M = 0, \text{ when: } T \le T_{\text{solidus}}$$

$$M = \frac{(T - T_{\text{solidus}})}{(T_{\text{liquidus}} - T_{\text{solidus}})}, \text{ when: } T_{\text{solidus}} < T < T_{\text{liquidus}}$$

$$M = 1, \text{ when: } T \ge T_{\text{liquidus}}$$

Where T_{solidus} and T_{liquidus} are the solidus and liquidus temperatures, respectively, which are specified for each rock type and dependent on the pressure (Table S2) (*Schmidt and Poli, 1998; Katz et al., 2003*).

5. Phase transitions

The phase transitions at 410 km and 660 km discontinuities are implemented in the numerical models (e.g., *Bina and Helffrich, 1994*), which modify the mantle density structure in addition to the gradual pressure and temperature dependence. The Clapeyron slope of phase transition at 410 km has a constant value of 3 MPa/K throughout this study, whereas the one at 660 km is varied with systematically testing its effects on subducting slab dynamics. The resulting density structure of the mantle is consistent with the Preliminary Reference Earth Model (PREM) (*Dziewonski and Anderson, 1981*). Two additional phase transitions are also implemented, i.e. the oceanic crustal eclogitization (*Ito and Kennedy, 2013*) and the metastable olivine in the MTZ (*Rubie and Ross, 1994*), with detailed algorithms summarized in *Li et al.* (2019).

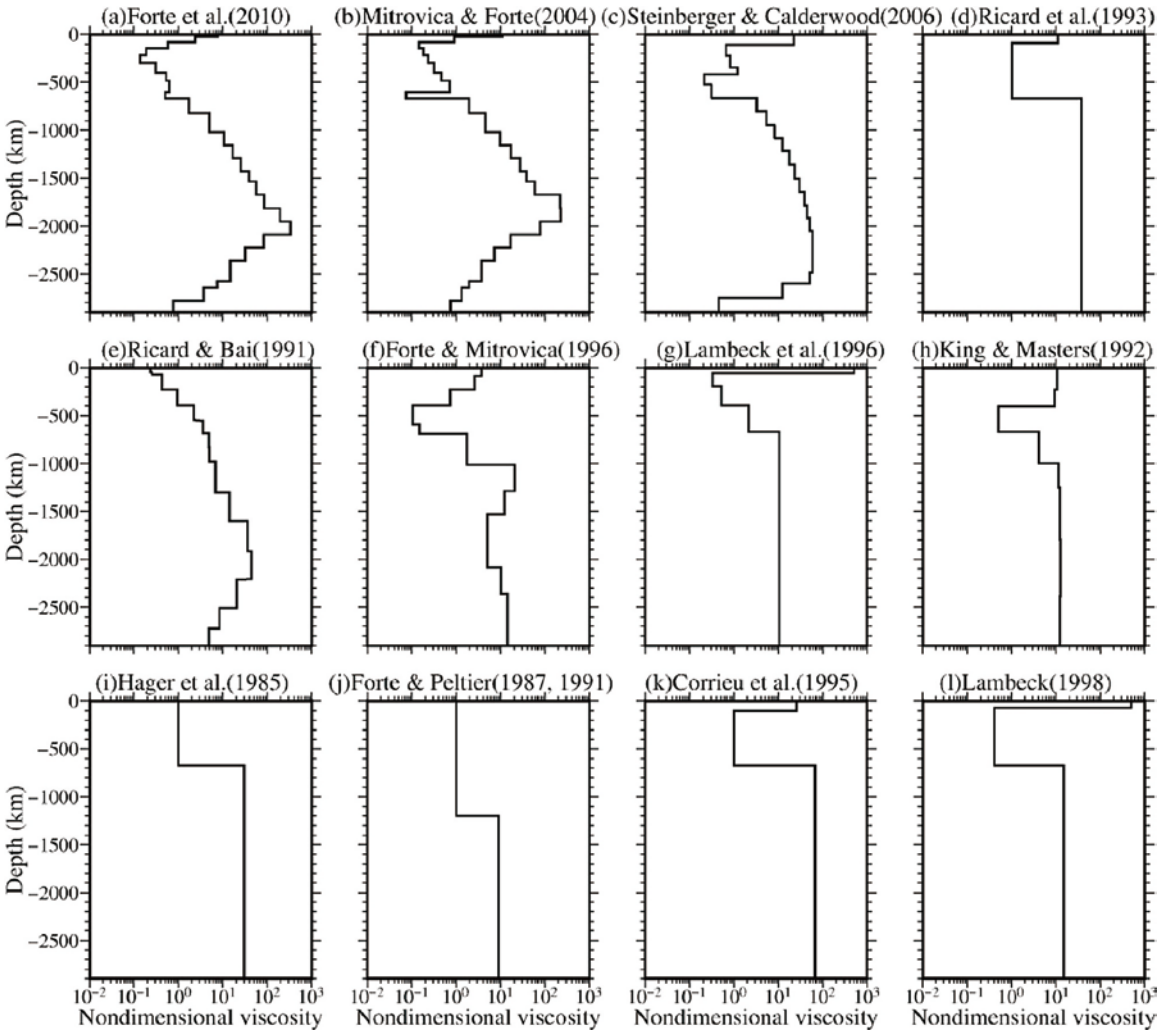

Figure S1. Previous inferences of depth-dependent effective mantle viscosity, as compiled by *Zhu* (2016). (a) and (b) are inferred from joint inversions of global convection-related observables and glacial isostatic adjustment (GIA) data (*Mitrovica and Forte, 2004; Forte et al., 2010*). (c) is inferred from mineral physics and surface observations (*Steinberger and Calderwood, 2006*). (d), (e) and (h)–(k) are derived on the basis of global long wavelength geoid anomalies (*Hager et al., 1985; Forte and Peltier, 1987, 1991; Ricard and Bai, 1991; King and Masters, 1992; Ricard et al., 1993; Corrieu et al., 1995*). (f), (g) and (l) are inferred mainly on the basis of GIA data (*Forte and Mitrovica, 1996; Lambeck et al., 1996, 1998*).

Table S1. Viscous flow laws used in the numerical experiments [a].

Symbol	Flow Law	E (kJ·mol^{-1})	V (J·MPa^{-1}·mol^{-1})	n	A_R (MPa^{-n}·s^{-1})	m	A_K (s^{-1})
A*	Wet quartzite	154	8	2.3	3.2×10^{-4}	-	-
B*	Plagioclase An_{75}	238	8	3.2	3.3×10^{-4}	-	-
C*	Dislocation creep of dry olivine	540	13	3.5	-	0.0	3.5×10^{22}
D*	Diffusion creep of dry olivine	300	4	1.0	-	2.5	8.7×10^{15}
E*	Dislocation creep of wet olivine	430	10	3.0	-	0.0	2.0×10^{18}
F*	Diffusion creep of wet olivine	240	4	1.0	-	2.5	5.3×10^{15}

[a] Viscous parameters of crustal rocks (A* and B*) are from *Kirby and Kronenberg* [1987] and *Ranalli* [1995]. Viscous parameters of mantle rocks (C*, D*, E*, F*) are from *Karato and Wu* [1993].

Table S2. Material properties used in the numerical experiments [a].

Material (state)	ρ_0 (kg·m^{-3})	C_p (J·kg^{-1}·K^{-1})	k [b] (W·m^{-1}·K^{-1})	$T_{solidus}$ [c] (K)	$T_{liquidus}$ [d] (K)	Q_L (kJ·kg^{-1})	H_r (μW·m^{-3})	**Viscous** [e] Flow law	**Plastic** [f] C_0 (MPa)	**Plastic** [f] $\sin(\varphi_{eff})$
Sediment (solid)	2600	1000	K_1	T_{S1}	T_{L1}	300	2.0	A*	10~1	0.1~0.05
Sediment (partial molten)	2400	1000	K_1	T_{S1}	T_{L1}	300	2.0	A*	10~1	0
Continental upper crust (solid)	2800	1000	K_1	T_{S1}	T_{L1}	300	1.0	A*	10~1	0.1~0.05
Continental upper crust (partial	2400	1000	K_1	T_{S1}	T_{L1}	300	1.0	A*	10~1	0
Continental lower crust (solid)	3000	1000	K_1	T_{S3}	T_{L3}	380	1.0	B*	10~1	0.1~0.05
Continental lower crust (partial	2400	1000	K_1	T_{S3}	T_{L3}	380	1.0	B*	10~1	0
Oceanic upper crust (solid)	3000	1000	K_2	T_{S2}	T_{L2}	380	0.25	A*	10~1	0.1~0.05
Oceanic upper crust (partial molten)	2900	1000	K_2	T_{S2}	T_{L2}	380	0.25	A*	10~1	0
Oceanic lower crust (solid)	3000	1000	K_2	T_{S3}	T_{L3}	380	0.25	B*	10~1	0.3~0.15
Oceanic lower crust (partial molten)	2900	1000	K_2	T_{S3}	T_{L3}	380	0.25	B*	10~1	0
Mantle (solid)	3300	1000	K_3	T_{S4}	T_{L4}	400	0.022	C*+D*	10~1	0.3~0.15
Mantle (hydrated)	3300	1000	K_3	T_{S4}	T_{L4}	400	0.022	E*+F*	10~1	0.1~0.05
Mantle (partial molten)	2900	1000	K_3	T_{S4}	T_{L4}	400	0.022	E*+F*	10~1	0
References [g]	1,2	1,2	3	6,7	6,7	1,2	1	4,5	-	-

[a] The thermal expansion coefficient $\alpha=2\times10^{-5}$ K^{-1} and the compressibility coefficient $\beta=0.75\times10^{-5}$ MPa^{-1} are used for all rock types.

[b] $K_1=[0.64+807/(T_K+77)]\cdot\exp(0.00004P_{MPa})$; $K_2=[1.18+474/(T_K+77)]\cdot\exp(0.00004P_{MPa})$; $K_3=[0.73+1293/(T_K+77)]\cdot\exp(0.00004P_{MPa})$.

[c] T_{S1}={889+17900/(P+54)+20200/(P+54)^2 at P<1200 MPa} or {831+0.06P at P>1200 MPa}; T_{S2}={973-70400/(P+354)+778×10^5/(P+354)^2 at P<1600 MPa} or {935+0.0035P+0.0000062P^2 at P>1600 MPa}; T_{S3}=1327+0.0906P; T_{S4}=KATZ2003.

[d] T_{L1}=1262+0.09P; T_{L2}=1423+0.105P; T_{L3}=1423+0.105P; T_{L4}=KATZ2003.

[e] Parameters of viscous flow laws are shown in Table S1.

[f] Strain weakening effect is included in plastic rheology, in which both cohesion C_0 and effective friction angle $\sin(\varphi_{eff})$ decrease with larger strain rate.

[g] References: 1-*Turcotte and Schubert* [2002]; 2-*Bittner and Schmeling* [1995]; 3-*Clauser and Huenges* [1995]; 4-*Ranalli* [1995]; 5-*Karato and Wu* [1993]; 6-*Schmidt and Poli* [1998]; 7-*Katz et al.* [2003].